# Registration uncertainty in deforming organs: A novel approach for ensuring navigational confidence during image-guided procedures

Jon S. Heiselman[1,2,3], William R. Jarnagin[1], and Michael I. Miga[2,3]

[1]Department of Surgery, Hepatopancreatobiliary Service, Memorial Sloan Kettering Cancer Center, New York, NY
[2]Department of Biomedical Engineering, Vanderbilt University, Nashville, TN
[3]Vanderbilt Institute for Surgery and Engineering, Vanderbilt University, Nashville, TN

## ABSTRACT

Successful estimation of target registration error (TRE) would provide immense opportunities for controlling risks associated with navigation during image-guided surgery. While developed theories exist for predicting spatial distributions of TRE for rigid point-based registration, similar capabilities in the domain of deformable registration are still needed to develop truly reliable image guidance systems for navigation in soft tissue organs. Recently, breakthrough work derived two analytic uncertainty metrics based on the dissipation of constraint energy over distance to measure the susceptibility of elastic deformable registration to errors originating from unknown effects that occur where registration constraints are missing. In this work, these registration uncertainties are leveraged to classify error thresholds for detecting spatial regions that become vulnerable to inaccuracy in sparse data driven elastic registrations. With a large dataset of over 6000 registrations, receiver operating characteristic (ROC) analysis was performed to assess discriminatory performance of these uncertainty metrics to clinically relevant levels of registration error and to identify optimal binary cutoffs for their prediction. Both uncertainty metrics were capable of detecting regions of the organ where deformable registration accuracy exceeded the average magnitude of rigid registration error with AUC above 0.87. Furthermore, both metrics detected regions of the organ with TRE greater than 10 mm with AUC of approximately 0.8. These new capabilities will enhance clinical confidence in image-guided technologies in deforming organs through enabling immediate quantification and communication of navigational reliability and system accuracy during soft tissue surgery.

**Keywords:** Registration, error, uncertainty, image guidance, navigation, deformation, soft tissue, surgery.

## 1. INTRODUCTION

The ability to predict registration error has been a longstanding need for ensuring the reliability of image-guided techniques in clinical practice. In soft tissue organs, the process of establishing a mapping between preoperative images and the intraoperative organ is usually affected by deformation, which presents a challenge when attempting to precisely correlate preoperative anatomy and disease with intraoperative presentation during medical intervention. While techniques exist for predicting average distributions of target registration error (TRE) for rigid body registration [1–5], methods that establish similar capabilities under conditions of deformation for nonrigid image-to-physical registration have been absent from the literature.

In recent work, Heiselman and Miga [6] demonstrated that it is indeed possible to predict the average magnitude and spatial distribution of registration errors associated with elastic registration techniques, whereby uncertainty measures were computed based on the dissipation of strain energy associated with equivalent boundary conditions collocated with the informational data constraints provided to the registration method. This work introduced two uncertainty measures for elastic deformable registration, one retrospective metric that utilized internal strain energy measures computed after registration had completed, and one prospective metric that utilized external energy approximations to enable more immediate computation prior to initiating registration. This work showed that the average value of the constraint uncertainty computed by each metric was able to independently predict average TRE across the registered organ to accuracy under 1.0

mm if the baseline magnitude of initial rigid registration error was known. Furthermore, pointwise values of uncertainty predicted TRE of clinical targets to below 3.5 mm accuracy using the median value of fitted statistical distributions that related uncertainty with registration error.

However, there remains a particular need for establishing realistic error thresholds for registration that are defined and evaluated with respect to clinical relevance. While the previous work by Heiselman and Miga [6] can predict the spatial distribution of TRE, these distributions were realized through median probabilities of relative errors whose interpretation requires an estimate of initial error prior to registration. When casting these findings towards clinical application, a gap persists in relating predicted registration errors to comprehensible references such as millimetric lengths compared to oncological margin or scale of improvement compared to conventional rigid registration approaches. In this paper, an alternative receiver-operating characteristic (ROC) analysis is performed on the data and methods introduced in [6] to address these limitations by testing whether the novel constraint uncertainty metrics can successfully distinguish clinically pertinent error thresholds to offer more relevant and useful feedback to the operating surgeon.

## 2. METHODS

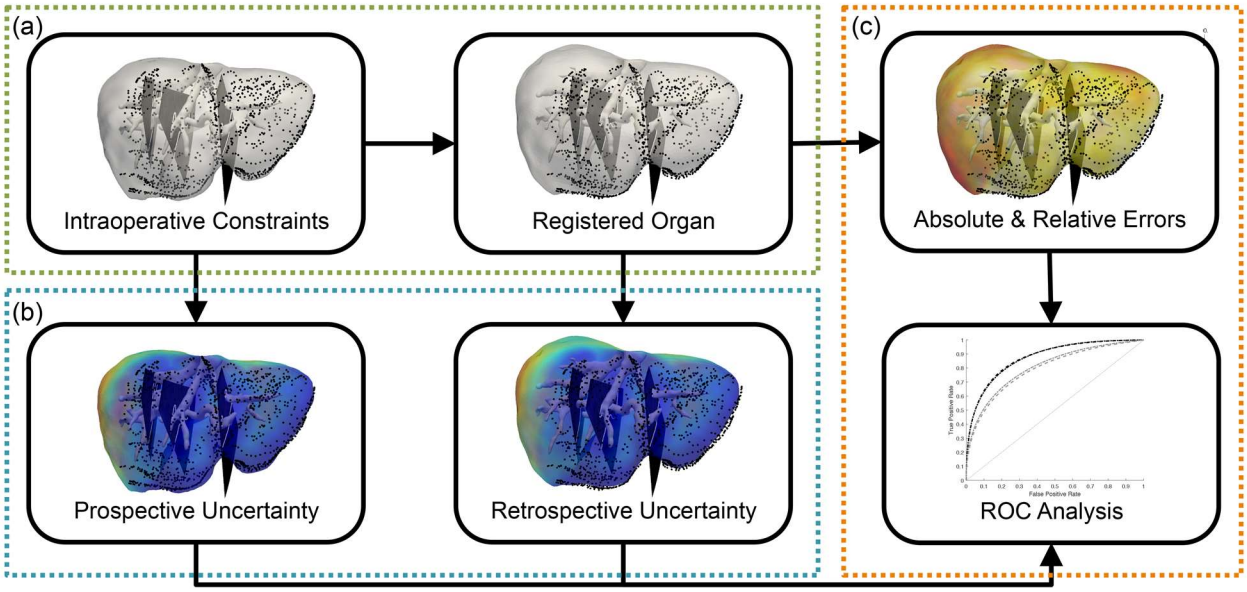


**Figure 1.** Overview of registration error prediction and analysis. (a) Deformable registration of preoperative organ anatomy (gray) to intraoperative data constraints (black). (b) Computation of registration uncertainty from intraoperative constraints and registration results. (c) Predictive analysis of registration errors.

### 2.1 Deformable Registration

The linearized iterative boundary reconstruction registration method and a large dataset of 6291 registration cases utilized in this study were first presented in [7]. Briefly, the dataset consists of three unique, patient-derived liver volumes each subjected to deformation fields mapped from the motions of 147 imaging targets that were embedded in a silicone organ phantom and re-imaged in three distinct states of mock laparoscopic deformation produced by varying degrees of mobilization of the hepatic ligaments. This process yielded nine different deformed organ states each with known ground truth nodal displacements. Clinical patterns of organ surface data obtained from an optically tracked stylus were mapped onto the anterior surfaces, and sixteen ultrasound planes and their intersections with the hepatic vasculature and the posterior capsular boundary were sampled from the deformed organ to generate sparse intraoperative data constraints for the registration method. These data were assembled in a combinatorial manner to produce 699 registration scenarios for each of the nine unique deformations. This phantom-to-human approach, inspired by the simulation framework of

Collins et al. [8], addresses a traditional barrier to the investigation of target error in deforming organs caused by a scarcity of clinically realistic datasets with known ground truth deformations and sufficient variation in the extent of data constraints.

With these generated data, the registration method begins with a salient feature weighted iterative closest point rigid registration [9] to provide a robust initial alignment of intraoperative data with the preoperative anatomy. Then, deformable registration is achieved using a linearized basis of elastic deformation responses precomputed over the preoperative organ domain to rapidly reconstruct external forces applied to the organ that best match the intraoperative deformation state by iteratively minimizing the difference between the deformed model and the provided registration constraints [7].

### 2.2 Registration Uncertainty

As presented in [6], uncertainty in elastic registration can be related to the distribution of data constraints provided to the registration algorithm by modeling the energetic dissipation of these constraints as their influence propagates over distance. In an elastic medium, the proportion of energy supplied by an applied load that reaches a particular location within the domain is bounded by the Toupin decay [10],

$$U(r) \leq U^0 e^{-kr}, \tag{1}$$

where $U(r)$ is the total energy that propagates beyond distance $r$ from the applied load, $U^0$ is the total energy of the excitation, and $k$ is a rate constant that depends on the material properties and the shape of the domain according to

$$k \propto \sqrt{\frac{\rho\omega_0}{\mu^*}}, \tag{2}$$

where $\rho$ is density, $\mu^*$ is an elastic modulus, and $\omega_0$ is the first characteristic frequency of free vibration. Precise details are provided in [6] for computing $k$ and $U^0$ from quantities measured after the registration has been performed (retrospective metric, $k_r$ and $U_r^0$), or alternatively prior to initiating registration (prospective metric, $k_p$ and $U_p^0$). Heiselman and Miga proposed that the constraint uncertainty at any location $x$ within the domain could be understood as the informational content of the total energy that reaches this position from the dominant closest constraint, according to

$$S(x) = -\ln\big(U(x)\big) \geq k\delta - \ln(U^0), \tag{3}$$

for $\delta = \min(\|x - x_c\|_2)$ where $x_c$ are the constraint positions. In this way, the retrospective and prospective constraint uncertainty measures

$$S_r(x) \geq k_r\delta - \ln(U_r^0), \tag{4}$$

$$S_p(x) \geq k_p\delta - \ln\big(U_p^0\big), \tag{5}$$

respectively, encode a lower bound on the amount of energetic attenuation the dominant constraint that originates at $x_c$ experiences before reaching position $x$. Consequently, these uncertainties measure the susceptibility of any location within the organ to be influenced by additional loads and unknown forces that are not accounted by the deformation constraints provided to the registration. Both uncertainty measures are nearly instantaneous to compute throughout an organ volume, and were evaluated for each of the 6291 registration cases.

### 2.3 Analysis of Error Prediction

This paper extends analysis of the data in [6] by evaluating the discriminatory power of the uncertainty metrics $S_r$ and $S_p$ over clinically relevant thresholds for absolute and relative error. In this work, ROC analyses are performed to evaluate how effectively the uncertainty metrics are capable of classifying these error levels based on binary thresholds for registration uncertainty. Each ROC curve is constructed from over

161 million paired samples of uncertainty measures and observed error values derived from ground truth knowledge of each volumetric mesh node in each of the 6291 unique registered cases.

In [6], it was found that the uncertainty metrics had superior correlation to relative errors as opposed to absolute millimetric errors. The relative error capacity $E$ at each position $x$ in the organ was defined as

$$E(x) = \frac{TRE_{nonrigid}(x)}{\text{mean}\left(TRE_{rigid}(x)\right)} * 100\% \tag{6}$$

where $TRE_{nonrigid}$ is the TRE after deformable registration and $TRE_{rigid}$ is the initial TRE associated with rigid registration. This normalization process effectively represents the proportion of error that still remains after deformable registration relative to the initial *average* uncorrected magnitude.

With respect to error thresholds, ordinarily 10 mm is considered a desirable standard for surgical margins of primary liver cancers [11–13]. Therefore, a 10-mm TRE threshold for identifying a clinical bound on registration uncertainty is reasonable. However, for the purposes of guiding around and transecting hepatic vasculature, accuracy thresholds corresponding to 5-mm or 3-mm would be desirable. With regard to relative error, if it can be assured that deformable registration will offer better accuracy than the average magnitude of error associated with rigid registration, then the deformable registration can be trusted to make an improvement over rigid registration within a specific range of uncertainties; hence, an error capacity of 100% is a desirable threshold. Error capacity thresholds of 50% and 30% are also included to identify uncertainty levels where below half or less than one third, respectively, of the initial magnitude of error remains. For each threshold, AUC and optimal operating cutoffs were computed for $S_r$ and $S_p$ metrics. To adjust for uneven class distribution, i.e. the number of samples with target errors below the threshold tends to be much greater than the number of samples with target errors exceeding the threshold, optimal operating cutoffs were defined by population-weighted cost balance [14], namely the intersection of the ROC curve with a negative diagonal of slope equal to the ratio of sub-threshold to super-threshold samples.

## 3. RESULTS

The evaluated error thresholds, optimal binary cutoffs, and areas under the curve (AUC) for both registration uncertainty metrics are shown in Table 1. AUC was found to exceed 0.87 for both uncertainty metrics when predicting relative errors of $E$ > 100%, indicating that either uncertainty measure is capable of excellent discrimination regarding precisely where in the organ TRE after deformable registration will fail to be lower than the average error associated with conventional rigid registration. Furthermore, AUC for predicting absolute $TRE$ > 10 mm was approximately 0.8 for both uncertainty metrics, indicating good performance when using the uncertainty metrics to detect egregiously high errors that may still exist after deformable registration. ROC curves corresponding to these error thresholds are shown in Figure 2. Figure 3 illustrates key examples of how these optimal uncertainty thresholds can be presented to highlight spatial regions where registration errors may surpass acceptable levels of performance.

| Error Threshold | Relevance | Optimal Cutoff, $S_r$ [AUC] | Optimal Cutoff, $S_p$ [AUC] |
|---|---|---|---|
| **$E$ > 100%** | **Improvement over Rigid** | **$S_r$ > 7.34 [0.874]** | **$S_p$ > 27.42 [0.873]** |
| $E$ > 50% | Initial Error Halved | $S_r$ > 5.35 [0.755] | $S_p$ > 20.10 [0.758] |
| $E$ > 30% | Initial Error 70% Reduced | $S_r$ > 4.10 [0.702] | $S_p$ > 14.93 [0.708] |
| **$TRE$ > 10 mm** | **Oncological Margin** | **$S_r$ > 6.39 [0.792]** | **$S_p$ > 24.05 [0.806]** |
| $TRE$ > 5 mm | Vascular Navigation | $S_r$ > 4.66 [0.695] | $S_p$ > 17.05 [0.712] |
| $TRE$ > 3 mm | Vascular Navigation | $S_r$ > 2.45 [0.672] | $S_p$ > 8.67 [0.689] |

**Table 1.** Error thresholds and optimal cutoffs for registration uncertainty metrics.

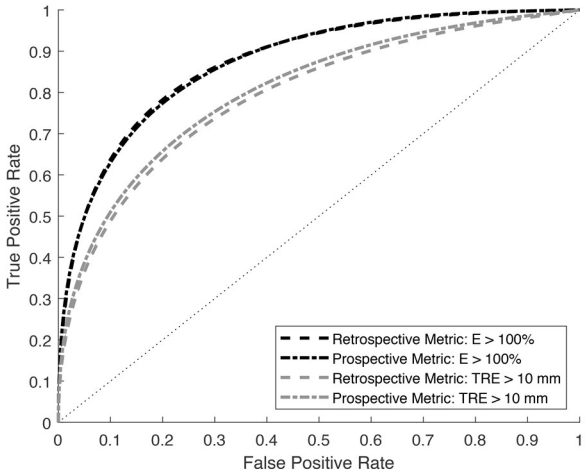


**Figure 2.** ROC curves for binary classification of error thresholds utilizing retrospective metric $S_r$ and prospective metric $S_p$ with respect to the bolded categories of Table 1.

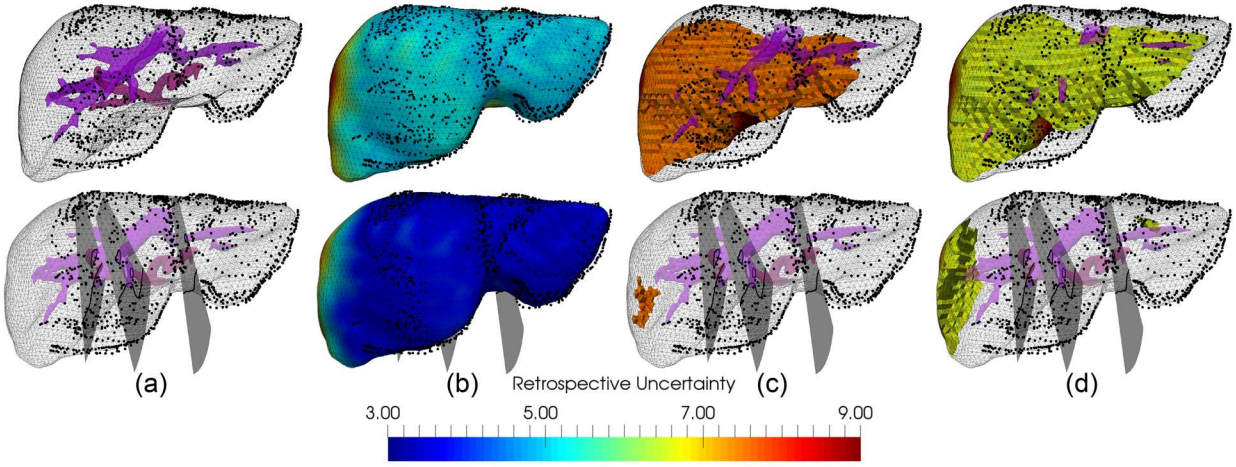


**Figure 3.** Organ regions exceeding critical error thresholds based on optimal cutoffs for retrospective uncertainty $S_r$. (a) Preoperative liver model (gray) and hepatic vasculature (purple) registered to intraoperative data constraints (black); top: registration to sparse anterior surface data only; bottom: registration to sparse anterior surface data plus additional constraints from intraoperative ultrasound image planes, including posterior surface and intrahepatic vascular features. (b) Retrospective uncertainty computed at every vertex of the registered organ models. (c) Highlighted region of the organ (orange) where uncertainty exceeds cutoff associated with $E > 100\%$. (d) Highlighted region of the organ (yellow) where uncertainty exceeds cutoff associated with $TRE > 10$ mm. Additional data constraints may be provided to the registration to improve projected accuracy.

## 4. DISCUSSION

In Table 1, predictive capabilities of both uncertainty metrics tended to be superior for relative errors ($E$) than absolute errors (TRE). It has long been observed that absolute levels of TRE achievable with nonrigid registration methods frequently depend on the initial magnitude of deformation. This dependence has led to the introduction of metrics such as percent correction in more comprehensive studies of deformable registration accuracy, especially when methods are evaluated across diverse ranges of initial errors. While

absolute errors are realistically the most vital to clinical practice, relative errors better convey the algorithmic effectiveness of deformable registration methods. However, intrinsic limitations surrounding error prediction at smaller scales cannot be ignored. Error floors impact nearly every registration method, where input noise from intraoperative data, modeling and numerical error, segmentation accuracy, and image resolution ultimately contribute to a minimum achievable TRE. While Table 1 seems to show diminished AUCs associated with uncertainty predictions across lower error thresholds, the overall predictive findings are still remarkable considering the aforementioned sources of error in addition to limitations regarding uncertainty computation in a domain where point-to-point correspondence cannot be certain.

Tradeoffs should also be noted in the choice of operating cutoff along the ROC curve. With respect to the clinical objective, true positive rate should be maximized to most conservatively avoid missed detection of high error regions. However, successful visualization of errors depends on minimizing false positive rate. These directions must contend simultaneously with statistical considerations of imbalanced class distribution that originate on the basis that effectual registration methods tend to generate disproportionately few regions of high registration error. For example, of the 161 million target error samples, only 8.5% were associated with $E > 100\%$ and 18.1% with $TRE > 10$ mm. This type of imbalance necessitates greater specificity through cutoffs with lower false positive rates. The optimal cutoff method described in Section 2.3 appropriately compensates for inter-class frequency bias. The cutoff values of both metrics associated with $E > 100\%$ and $TRE > 10$ mm reported in Table 1 correspond to specificity values of 99% and 97%, respectively. Operating on the left side of the ROC curve is reasonable because regions of high error will tend to remain spatially collocated, and therefore perfect sensitivity is not needed for detection of bulk regions of elevated error. However, the spatial precision of the error boundaries shown in Figure 3 may deteriorate at cutoffs associated with smaller true positive rate. These factors contribute to an overall limitation with respect to determining a cutoff choice that satisfies all considerations. It must also be recognized that binary classifiers fundamentally struggle with imprecision in the "gray area" around the decision threshold, and therefore the predicted error boundaries obtained from this approach should only be treated as spatially approximate. Additionally, the best operating cutoff also depends on the underlying accuracy and variability of the specific registration method. While prospective testing is needed to fully validate the reported uncertainty thresholds, AUC values indicate that the registration uncertainty metrics are suitable for predicting regions of high registration error.

In all, this work reports a novel approach for analyzing registration uncertainties associated with error propagation in elastic deformable registration. ROC analysis was performed to test the capability of these uncertainty measures with respect to critical thresholds on absolute TRE and relative error capacity. While the derivation of uncertainty metrics and the dataset utilized in this work were recently published in IEEE Transactions on Medical Imaging [6], to enhance clinical relevance, this paper extends the analysis of the already published work by measuring accuracy characteristics of error prediction using these uncertainty metrics according to clinically relevant error thresholds. As such, the analysis presented herein is quite novel and represents the first work to predictively detect and classify severe regions of registration error from uncertainty measures in elastically deformable registration.

## 5. CONCLUSION

The ability to predict registration errors associated with deformable registration has long been sought. Recently, uncertainty metrics based on the spatial dissipation of constraint energy have come forth that correlate the spatial distribution of registration constraints with resulting registration error. This work shows that these uncertainty metrics are also highly effective at classifying specific thresholds of relative and absolute registration errors. These capabilities achieve an intraoperative system for registration assurance that can detect perilous levels of error during image-guided navigation. Complete realization of these methods will enable highly reliable image guidance systems with embedded certainty and control that should become a foundational prerequisite for nurturing the confidence necessary to build more widespread clinical adoption of deformable registration techniques in image-guided soft tissue procedures.

## ACKNOWLEDGMENTS

This work was supported in part by NIH-NIBIB grant number R01EB027498.

## REFERENCES

[1] J. M. Fitzpatrick, J. B. West, and C. R. Maurer, "Predicting error in rigid-body point-based registration," *IEEE Trans. Med. Imaging*, vol. 17, no. 5, pp. 694–702, 1998.

[2] J. M. Fitzpatrick and J. B. West, "The distribution of target registration error in rigid-body point-based registration," *IEEE Trans. Med. Imaging*, vol. 20, no. 9, pp. 917–927, 2001.

[3] A. D. Wiles, A. Likholyot, D. D. Frantz, and T. M. Peters, "A statistical model for point-based target registration error with anisotropic fiducial localizer error," *IEEE Trans. Med. Imaging*, vol. 27, no. 3, pp. 378–390, 2008.

[4] M. H. Moghari and P. Abolmaesumi, "Distribution of target registration error for anisotropic and inhomogeneous fiducial localization error," *IEEE Trans. Med. Imaging*, vol. 28, no. 6, pp. 799–813, 2009.

[5] A. Danilchenko and J. M. Fitzpatrick, "General approach to first-order error prediction in rigid point registration," *IEEE Trans. Med. Imaging*, vol. 30, no. 3, pp. 679–693, 2011.

[6] J. S. Heiselman and M. I. Miga, "Strain energy decay predicts elastic registration accuracy from intraoperative data constraints," *IEEE Trans. Med. Imaging*, vol. 40, no. 4, pp. 1290–1302, 2021.

[7] J. S. Heiselman, W. R. Jarnagin, and M. I. Miga, "Intraoperative correction of liver deformation using sparse surface and vascular features via linearized iterative boundary reconstruction," *IEEE Trans. Med. Imaging*, vol. 39, no. 6, pp. 2223–2234, 2020.

[8] J. A. Collins, J. A. Weis, J. S. Heiselman, L. W. Clements, A. L. Simpson, W. R. Jarnagin, and M. I. Miga, "Improving registration robustness for image-guided liver surgery in a novel human-to-phantom data framework," *IEEE Trans. Med. Imaging*, vol. 36, no. 7, pp. 1502–1510, 2017.

[9] L. W. Clements, W. C. Chapman, B. M. Dawant, R. L. Galloway, and M. I. Miga, "Robust surface registration using salient anatomical features for image-guided liver surgery: algorithm and validation," *Med. Phys.*, vol. 35, no. 6, pp. 2528–2540, 2008.

[10] R. A. Toupin, "Saint-Venant's principle," *Arch. Ration. Mech. Anal.*, vol. 18, no. 2, pp. 83–96, 1965.

[11] K. Lafaro, M. S. Grandhi, J. M. Herman, and T. M. Pawlik, "The importance of surgical margins in primary malignancies of the liver," *J. Surg. Oncol.*, vol. 113, no. 2016, pp. 296–303, 2016.

[12] H. Nitta, M.-A. Allard, M. Sebagh, N. Golse, O. Ciacio, G. Pittau, E. Vibert, A. Sa Cunha, D. Cherqui, D. Castaing, H. Bismuth, H. Baba, and R. Adam, "Ideal surgical margin to prevent early recurrence after hepatic resection for hepatocellular carcinoma," *World J Surg*, vol. 45, pp. 1159–1167, 2021.

[13] F. Zhong, Y. Zhang, Y. Liu, and S. Zou, "Prognostic impact of surgical margin in patients with hepatocellular carcinoma: A meta-analysis," *Medicine (Baltimore).*, vol. 96, no. 37, p. e8043, 2017.

[14] J. P. Marques de Sá, *Applied Statistics Using SPSS, STATISTICA, MATLAB, and R*, 2nd ed. Springer Science and Business Media, Inc., 2007, pp. 250–251.